Morphologies in solvent-annealed thin films of symmetric diblock copolymer

Juan PengDong Ha KimWolfgang KnollYu Xuan, Binyao Li, and Yanchun Han

Citation: The Journal of Chemical Physics **125**, 064702 (2006); doi: 10.1063/1.2219446
View online: http://dx.doi.org/10.1063/1.2219446
View Table of Contents: http://aip.scitation.org/toc/jcp/125/6
Published by the American Institute of Physics

Morphologies in solvent-annealed thin films of symmetric diblock copolymer

Juan Peng[a)]
State Key Laboratory of Polymer Physics and Chemistry, Changchun Institute of Applied Chemistry, Graduate School of the Chinese Academy of Sciences, Chinese Academy of Sciences, Changchun 130022, People's Republic of China

Dong Ha Kim
Max Planck Institute for Polymer Research, Ackermannweg 10, 55128 Mainz, Germany and Division of Nano Sciences and Department of Chemistry, Ewha Womans University, 11-1 Daehyun-Dong, Seodaemun-Gu, Seoul 120-750, Korea

Wolfgang Knoll
Max Planck Institute for Polymer Research, Ackermannweg 10, 55128 Mainz, Germany

Yu Xuan, Binyao Li, and Yanchun Han[b)]
State Key Laboratory of Polymer Physics and Chemistry, Changchun Institute of Applied Chemistry, Graduate School of the Chinese Academy of Sciences, Chinese Academy of Sciences, Changchun 130022, People's Republic of China

(Received 19 December 2005; accepted 7 June 2006; published online 8 August 2006)

We have systematically studied the thin film morphologies of symmetric poly(styrene)-block-poly(methyl methacrylate) (PS-*b*-PMMA) diblock copolymer after annealing to solvents with varying selectivity. Upon neutral solvent vapor annealing, terraced morphology is observed without any lateral structures on the surfaces. When using PS-selective solvent annealing, the film exhibits macroscopically flat with a disordered micellar structure. While PMMA-selective solvent annealing leads to the dewetting of the film with fractal-like holes, with highly ordered nanoscale depressions in the region of undewetted films. In addition, when decreasing the swelling degree of the film in the case of PMMA-selective solvent annealing, hills and valleys are observed with the coexistence of highly ordered nanoscale spheres and stripes on the surface, in contrast to the case of higher swelling degree. The differences are explained qualitatively on the basis of polymer-solvent interaction parameters of the different components. © *2006 American Institute of Physics*.
[DOI: 10.1063/1.2219446]

I. INTRODUCTION

Block copolymers are composed of covalently bonded sequences of chemically distinct repeated units. Because of the incompatibility, block copolymers usually microphase separate into well-ordered nanoscale structures below an order-disorder transition temperature.[1–3] The segregation strength is primarily determined by the enthalpy and entropy reasons and usually scaled by χN, the product of the Flory-Huggins parameter (χ) between the blocks and the total degree of polymerization (N) of the copolymer. For symmetric diblock copolymers, microphase separation is expected at $\chi N > 10.5$ according to theoretical prediction.[4] Depending on the volume fraction of components, lamellae, gyroids, cylinders, and spheres have been observed.[1–4]

When block copolymers are confined to the surface of a solid substrate, preferential interactions of the blocks with the substrate and differences in the surface energies of the blocks will force the orientation of lamellae or cylinders parallel to the film surface. For the symmetric diblock copolymers, this alignment often leads to a "thickness quantization" of the thin film. When the thickness of film is not commensurate to the equilibrium lamellar spacing, either holes or islands are nucleated on the film surface to adjust the local film thickness to the preferred quantized values.[5]

While a large number of studies have been reported on thermally equilibrated block-copolymer morphologies, there is a growing interest in researching the evolution of microstructure and transformation between various phases in response to solvent swelling.[6–21] Though the preparation process usually leads to the formation of metastable structures that do not represent the melt equilibrium, such structures often exhibit high regularity and may be of particular interest for patterning applications as they significantly increase the number of patterns to be created by a given polymer.

For a given *A*-*B* block copolymer, a solvent can be classified as neutral or selective, depending on the extent to which it preferentially swells the microdomains of the copolymer morphology.[22–24] In general, neutral solvents are distributed nearly uniformly between A/B microdomains and decrease the A/B interaction parameter (χ). In other words,

[a)]Present address: Max Planck Institute for Polymer Research, Ackermannweg 10, 55128 Mainz, Germany. Electronic mail: peng@mpip-mainz.mpg.de
[b)]Author to whom correspondence should be addressed; FAX: 86-431-5262126; electronic mail: ychan@ciac.jl.cn

neutral solvents can shield the unfavorable contact of blocks. In *A*-selective solvent, the *A* blocks are swollen while the *B* block adopt a collapsed conformation. These investigations on the solvent selectivity effects, to our knowledge by far, have tended to focus on either the melt[23] or dilute solutions,[25–27] where the selectivity drives micellization in the latter. The effects of solvent selectivity on the solvent-annealed block copolymer thin films, however, have been less studied.

In our previous report, we showed that by poly(methyl methacrylate) (PMMA)-selective solvent swelling, a series of nanostructures developing from highly ordered nanoscale depressions to stripes[18–20] or from highly ordered nanoscale spheres to stripes[21] can be obtained in symmetric poly(styrene)-block-poly(methyl methacrylate) (PS-*b*-PMMA) diblock copolymer thin films by tuning the film thickness, the solvent selectivity, the swelling degree of films, and solvent annealing time. The nanostructure is a potential candidate for future applications, it can, e.g., serve as template for nanopatterning after selective removal of one of the components without losing its order.

The present work is of interest in the effect of solvent selectivity on the solvent-annealed block copolymer thin films. We first will show that quite different thin film structures are formed in symmetric PS-*b*-PMMA thin films after solvent annealing depending on the nature of the solvent. Three solvents are chosen from neutral to different block selectives. In addition, we are specifically interested in comparing the thin film morphologies with different swelling degrees after PMMA-selective solvent annealing. In the case of higher swelling degree, fractal-like holes are formed with nanoscale depressions in the undewetted region. While in the case of lower swelling degree, hills and valleys are observed, on which nanoscale spheres and stripes are observed. The formation mechanisms of different film morphologies have been discussed in detail.

II. EXPERIMENT

A. Materials and sample preparation

The symmetric PS-*b*-PMMA diblock copolymer used in this study was obtained from Polymer Source, Inc, with total molecular weight M_w of 263 000 (M_{PS}=130 000 and M_{PMMA}=133 000) and polydispersity index M_w/M_n=1.07. For this copolymer, the lamellar period L_0 was measured to be approximately 90 nm (Ref. 28) (81 nm calculated from the empirical relation[29]). The diblock copolymer was dissolved in toluene (over 24 h to reach sufficient dissolution) with a typical concentration of 0.5 wt %. Thin polymer films (~22 nm) were then prepared by spin coating the toluene solution onto the silicon wafers with a layer of SiO_x (~2 nm thick from ellipsometry). Prior to spin coating, the wafers were cleaned with a 70/30 v/v solution of 98% H_2SO_4/30% H_2O_2 at 80 °C for 30 min, and then thoroughly rinsed with de-ionized (DI) water and dried. Film thickness was determined by an ellipsometry (AUEL-III, Xi'an, China).

B. Sample treatment

Without removing the residual solvent, the films were exposed to three different solvent vapors [tetrahydrofuran (THF), carbon disulfide (CS_2), and acetone] by placing them some millimeters above the liquid surface of the respective solvent kept in a vessel. The vessel is 790 cm^3 volume with plenty of solvent. In the case of acetone vapor annealing, some samples were also placed into a vessel with 20 cm^3 volume and 50 μl solvent. As we know, solvent adsorbs heat from the surrounding environment to change from liquid state to gas state, resulting in a decrease of system temperature. Accordingly, the solvent vapor pressure is varied. In turn, the degree of swelling of the polymer films is different. Obviously, the influences on the samples in the small vessel are much larger than those on the samples in the larger one. Therefore, it is assumed that the swelling degree of polymer films by acetone vapor is lower in small vessel than those in larger one.[21] All the experiments were performed at room temperature (~22 °C). After a certain exposure time, the sample was removed to ambient atmosphere and promptly dried.

C. Atomic force microscopy (AFM) characterization

The surface morphology was observed at ambient conditions by a commercial AFM, using a SPA-300HV with a SPI3800N controller (Seiko Instruments, Inc., Japan) in the tapping mode. The dry samples were mounted on a sample stage which was three-dimensionally driven by a piezotube scanner. Both height and phase images were recorded simultaneously. A silicon microcantilever (spring constant of 2 N/m and resonance frequency of ~70 kHz, Olympus, Japan) with an etched conical tip (radius of curvature of ~40 nm as characterized by scanning over very sharp needle array, NT-MDT, Russia) was used for scan. The A_{sp}/A_0 value was set to 0.90, where A_0 is the free oscillation amplitude and A_{sp} is the set point amplitude. The scan rate was in the range of 1.0–2.0 Hz.

In tapping mode, as the tip probes mechanically different domains, the phase contrast originates from local differences in tip-surface interactions. These interactions depend not only on the intrinsic properties of the analyzed material, in particular, its elastic modulus, but also on the mechanical properties of the tip and on the existence of tip-sample adhesion.[30] In the case of "soft-tapping" regime we used, that is, when the amplitude of the oscillating cantilever is only slightly reduced (for instance, for A_{sp}/A_0=0.90) upon interaction with the surface, it has been shown that the magnitude of the phase shift is directly related to the elastic modulus of the sample.[30–32] When probing a region of higher modulus, the force interaction leads to a more positive phase shift and hence appears brighter in a phase image.

D. Optical microscopy (OM) characterization

Optical images were obtained using a Leica optical microscopy (Leica Microsystems, Germany) in reflection mode with a charge-coupled device (CCD) camera attachment.

TABLE I. Polymer-solvent interaction parameters ($\chi_{P\text{-}S}$) calculated from different polymer-solvent pairs.

	THF	CS_2	Acetone
PS	0.34	0.43	1.1
PMMA	0.88	1.2	0.29

III. RESULTS

The miscibility between a polymer and a solvent can be governed by the polymer-solvent interaction parameter, $\chi_{P\text{-}S}$ (P=polymer and S=solvent).[33] For nonpolar systems, $\chi_{P\text{-}S}=V_S(\delta_S-\delta_P)^2/RT+0.34$, where V_S is the molar volume of the solvent, R is the gas constant, T is the temperature, and δ_S and δ_P are the solubility parameters of the solvent and polymer, respectively. For polar systems, $\chi_{P\text{-}S}=V_S[(\delta_{dS}-\delta_{dP})^2+(\delta_{pS}-\delta_{pP})^2]/RT$,[17] where δ_d is the dispersion solubility parameter and δ_p is the polar solubility parameter. By calculation, the $\chi_{P\text{-}S}$ values for different polymer-solvent pairs at room temperature (22 °C) are listed in Table I. According to Flory-Huggins theory, the polymer and solvent are completely miscible over the entire composition range when $\chi_{P\text{-}S}<0.5$. Thus, acetone is a selective solvent for PMMA, while CS_2 is PS selective. Though $\chi_{\text{PMMA-THF}}>0.5$, THF is a good solvent for both PS and PMMA blocks, exhibiting only a small selectivity to PS.[33,34] In fact, there are no truly neutral solvents for real block copolymer systems. The so-called neutral solvents always show some preferential affinity to one of the blocks.[24]

Solvent vapors of varying selectivity for the two blocks change film boundary and thus change the surface morphology. Following we will show that upon solvent vapor treatment, the PS-*b*-PMMA film morphologies are quite dependent on the solvent selectivity for the two blocks. In addition, we are specifically interested in comparing the thin film morphologies with different swelling degrees after PMMA-selective solvent annealing. The formation mechanisms of different film morphologies have been discussed in detail.

A. Neutral THF vapor annealing

The as-cast PS-*b*-PMMA thin films show a disordered wormlike pattern [Figs. 1(a) and 1(b)] due to the fast solvent evaporation making the chains have no enough time to rearrange to attain equilibrium morphology. On exposure to THF vapor for 23 h, the surface develops a stepped morphology [Fig. 2(a)]. From a set of cross sections taken at different positions of the sample, we find the step height is ~10 nm, which is far less than the bulk lamellar spacing. One reason is that constraints in the thin film induced by the boundary surfaces may suppress the establishment of the equilibrated lamellar microphase in the first-stage ordering process induced by the short-term solvent vapor exposure.[7] The surfaces of the terraces do not show any lateral structures, indicating the formation of lamellae aligned parallel to the plane of the film. This finding resembles the well-known surface-induced alignment of the lamellar microdomains observed on thermally equilibrated thin films of symmetric diblock copolymers.[35] Though THF turns out to be good solvent for both blocks, the observed morphology is kinetically trapped instead of an equilibrium structure.

B. PS-selective CS_2 vapor annealing

Now we present the morphologies of the PS-*b*-PMMA films annealed by CS_2 vapor. After exposing the film to CS_2 vapor for 23 h, the film remains flat and complete as the as-cast film in optical microscopy. AFM is used to reveal the structure of the film surface on a molecular length scale. Compared with the disordered wormlike pattern of the as-cast film, the film annealed by CS_2 vapor exhibits disordered micellar structure [Fig. 2(b)]. Since CS_2 is a good solvent for PS but a poor solvent for PMMA chains, PMMA blocks form aggregates with neighboring PMMA blocks to decrease contact with solvent, while PS blocks form a shield around the PMMA aggregates to avoid the PMMA-solvent unfavorable contact. Both effects lead to the formation of micellar structure.

C. PMMA-selective acetone vapor annealing

In the following, we concentrate on the surface morphologies of the PS-*b*-PMMA films after treatment with acetone vapor. Two different types of macroscopic morphologies are observed in the films with various swelling degrees

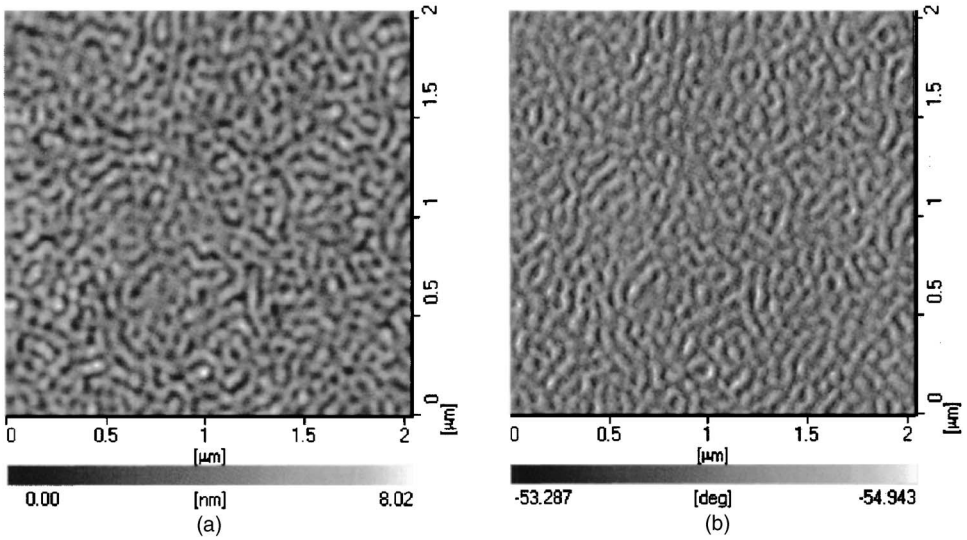

FIG. 1. AFM (a) height and (b) phase contrast images of an as-cast PS-*b*-PMMA thin film from toluene solution with a typical concentration of 0.5 wt %.

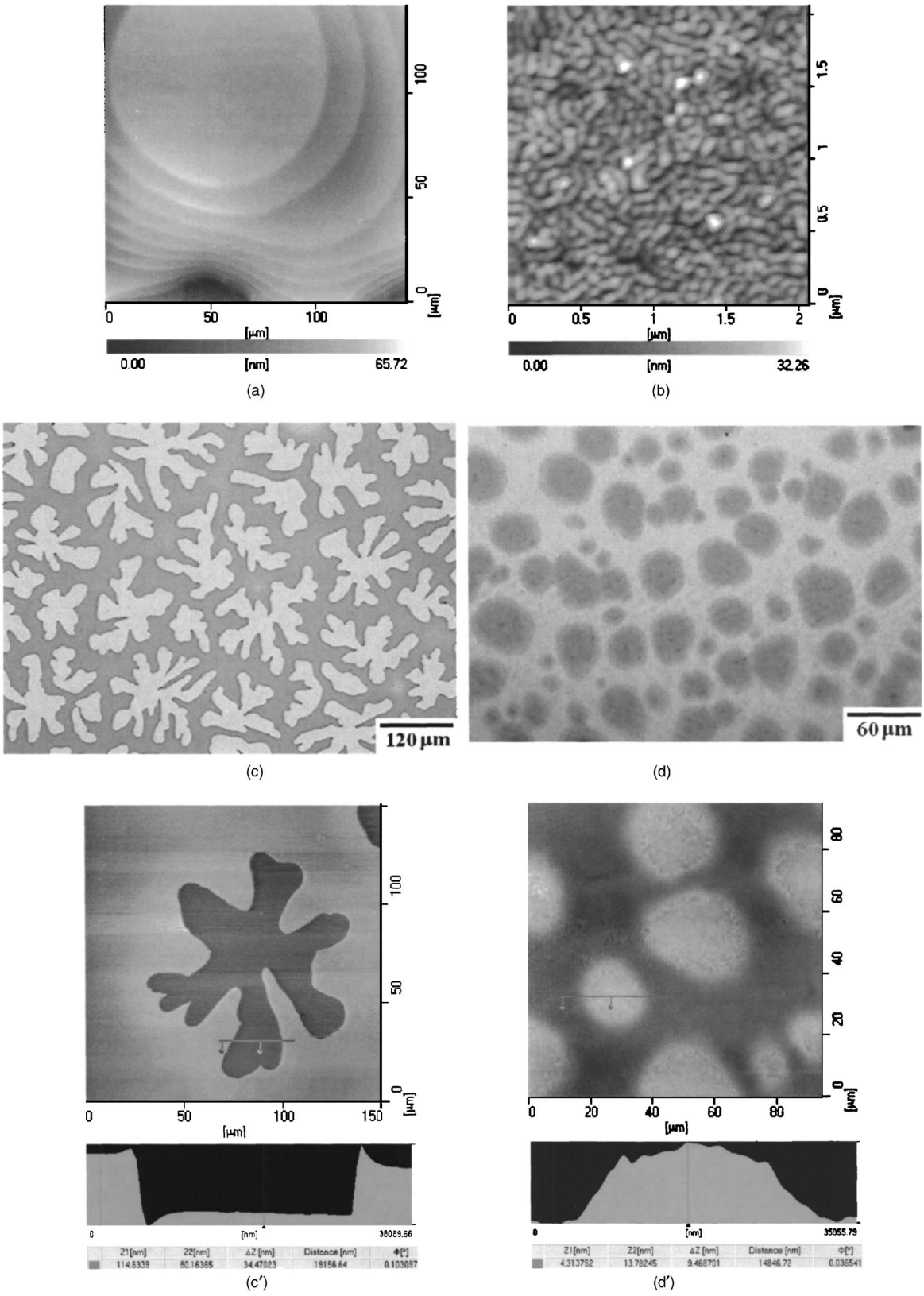

FIG. 2. AFM images and optical micrographs of the as-cast PS-*b*-PMMA thin films treated in (a) neutral THF vapor for 23 h, (b) PS-selective CS_2 vapor for 23 h, (c) PMMA-selective acetone vapor (higher swelling degree), and (d) lower swelling degree for 26 h. (c′) and (d′) are the AFM height images and cross sectional images of the corresponding (c) and (d).

[Figs. 2(c) and 2(d)]. We first discuss the films with higher swelling degree annealed by acetone vapor in larger vessel. Figure 2(c) shows an OM image of a PS-*b*-PMMA film after treatment with acetone vapor for 26 h. In the OM image, holes appear lighter than the surrounding areas of the films. Fractal-like holes are observed all over the surface. Figure 2 (c′) shows an AFM height image of a developed fractal-like hole with a depth of ~34 nm. An ultrathin film of the co-

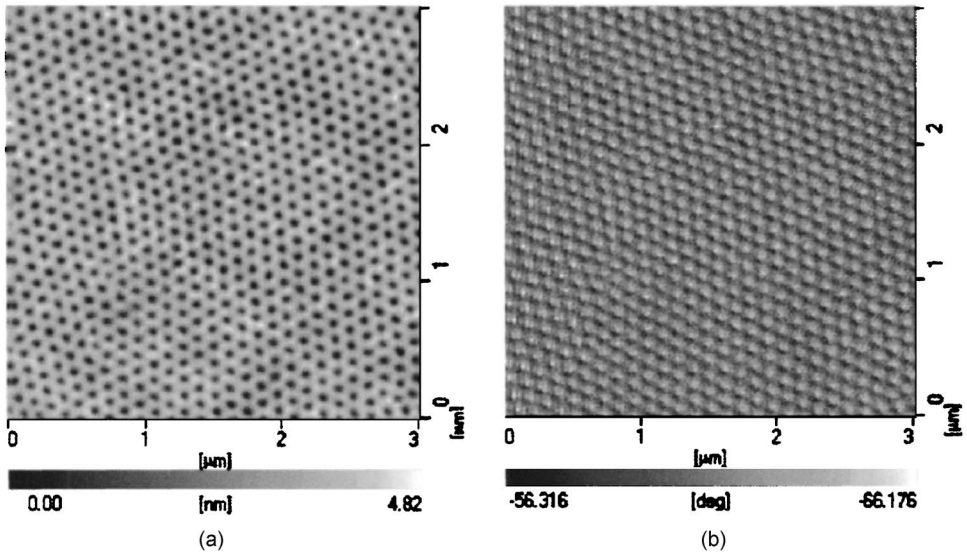

FIG. 3. AFM (a) height and (b) phase contrast images of the nanostructure in the region of undewetted PS-*b*-PMMA film in the case of higher acetone vapor swelling.

polymer is left behind in dewetted holes, which is attributed to a dense layer of ordered copolymer due to the strong attraction between PMMA chains and the native silicon oxide layer on the substrate.[36] The nanostructures on the region of undewetted film is magnified in Fig. 3, which exhibits ordered nanoscale depressions with the size of ~45 nm and the depth of ~3.5 nm. Its corresponding phase contrast image is shown in Fig. 3(b). Since PMMA has a higher modulus than PS chain at room temperature (bulk elastic moduli of PS and PMMA are 3.0 and 3.3 GPa, respectively[33]), we assign the brighter spots in AFM phase contrast image, which correspond to a larger phase shift, to domains of the PMMA of higher modulus, while the darker matrix, showing a smaller phase shift, is made of the PS of lower modulus. This assignment has been confirmed by transmission electron microscopy (TEM) experiments,[18,20] and is consistent with the observation in previous reports.[37,38] In TEM images, contrast between PS and PMMA derives from electron-irradiation-induced thinning of the PMMA (which thus appears brighter in the image). It shows that well-ordered PMMA cylinders are embedded in PS matrix. Our previous study showed with further annealing, the nanoscale depressions would transform into striped morphology.[18]

We then discuss the PS-*b*-PMMA films with lower swelling degree annealed by acetone vapor. Figure 2(d) shows an OM image of a PS-*b*-PMMA film after treatment with acetone vapor for 26 h. In contrast to the dewetted fractal-like holes observed in the case of higher swelling degree, in this case, hills and valleys are observed in PS-*b*-PMMA films. Figure 2(d′) shows an AFM height image of a smaller region, with an accompanying line scan showing that the hills are ~9 nm above the valleys. When scanning a smaller area, striped morphology is observed on the hills with the lamellar spacing of ~104 nm [Figs. 4(a) and 4(b)]. In the valleys, a hexagonally ordered nanoscale sphere structure is clearly manifested with the size, interval, and a height of 83, 31, and ~11.4 nm, respectively [Fig. 4(c)]. Its corresponding phase contrast image is shown in Fig. 4(d), which shows that spherical PS microdomains are embedded in PMMA matrix. Our previous research showed with further acetone vapor swelling, the spherical domains merge with each other and form elongated striped domains, which is energetically favored.[21]

IV. DISCUSSION

The experimental results can be summarized as follows. Upon THF vapor annealing, terraced morphology is observed without detecting any lateral structures on terrace surface, indicating lamella oriented parallel to the surfaces. Upon CS_2 vapor annealing, the film remains macroscopically flat with disordered micellar nanostructures on the surface. Upon acetone vapor annealing, higher swelling degree results in the dewetting of the PS-*b*-PMMA film with fractal-like holes, with nanoscale depressions in the region of undewetted films. Lower swelling degree, on the other hand, leads to the formation of hills and valleys, with the coexistence of nanoscale spheres and stripes on the film surface. The possible structure of the as-cast film and films subsequently annealed by different solvent vapors is schematically shown in Fig. 5.

We first turn to the differences in surface morphologies observed after THF, CS_2, and acetone vapor swellings. This difference can be understood by considering the polymer-solvent interaction parameter ($\chi_{P\text{-}S}$) values for different polymer-solvent pairs. Previous description has shown that when symmetric PS-*b*-PMMA is cast on a Si substrate with a SiO_x surface layer, PMMA is preferentially attracted to the silicon because it is the more polar component, and PS preferentially goes to the free surface because of its lower surface energy.[39] X-ray photoelectron spectroscopy (XPS) measurement showed that the surface PMMA weight fraction was 28.0%, relative to its fraction in the block copolymer (49%), indicating the PS preferentially, but not exclusively, segregates to the air interface [Fig. 5(a)].[21] When exposed to solvent vapor, the film is covered with solvent molecules. The film boundary condition is different from that in the air or in a vacuum. Furthermore, different solvent vapors of varying selectivities for the two blocks result in different film boundary conditions. During solvent swelling, it will be en-

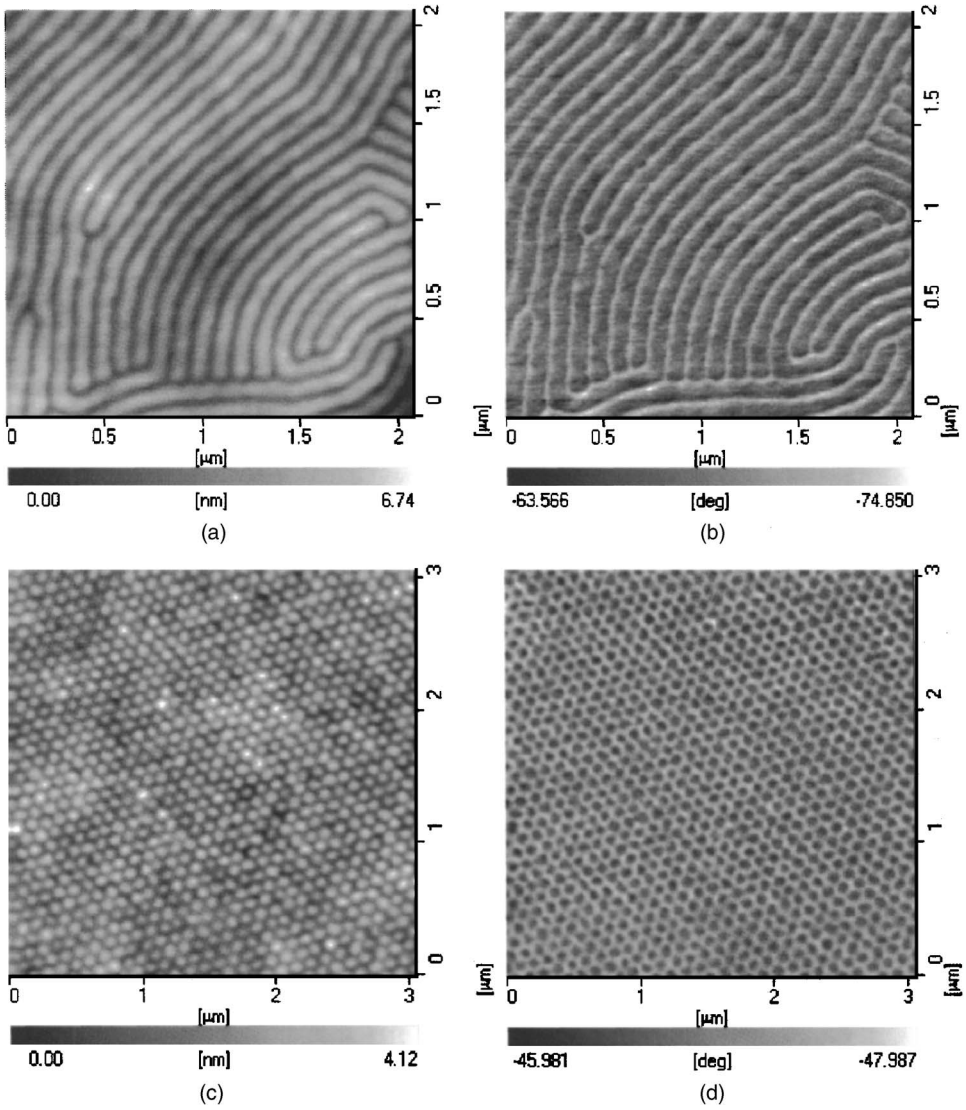

FIG. 4. [(a) and (c)] AFM height and [(b) and (d)] phase contrast images of the nanostructures in the PS-*b*-PMMA in the case of lower acetone vapor swelling. (a) and (b) on the hills, and (c) and (d) in the valleys.

ergetically favorable to cover the free surface of the diblock copolymer film by a continuous layer of the lower surface energy component. Since THF is a good solvent for PS and PMMA blocks, PS and PMMA are equally swollen by THF. The lamellar structure is formed by the external interfaces with SiO_x attracting the PMMA blocks and the free surface attracting the PS blocks [Fig. 5(b)]. In the presence of selective solvent vapor, CS_2 and acetone preferentially segregate into the PS and PMMA domains, respectively, due to the more favorable enthalpy of mixing. PS and PMMA are unequally swollen, which results in kinetic barriers for the chain transport necessary to achieve equilibrium morphology. Therefore, metastable morphologies form and are frozen after solvent removal. When treated in PS-selective CS_2 solvent, the PS blocks form a shield around the PMMA aggregates to avoid the PMMA-solvent unfavorable contact, resulting the micellar morphology [Fig. 5(c)]. Since the upper boundary condition still favors the PS, and the PS will continue to dominate the upper surface. The solvents disturb the film less and thus the film remains stable.

In the following we focus on the different macroscopic structures by similar acetone vapor swelling. In the case of higher swelling degree, the driving forces for the dewetting of PS-*b*-PMMA films on the silicon oxide is the strong tendency of acetone molecules to attract the bottom PMMA uprising. We have pointed out due to the presence of asymmetric boundary condition, PMMA preferentially segregates to the SiO_x substrate and the PS segregates to the air interface. On exposure to acetone vapor, a selective solvent for PMMA, it turns into symmetric boundary condition. Solvent vapor molecules have a strong tendency to attract PMMA to maximize the PMMA-solvent contacts. So PMMA is pulled toward the film surface. The movement of PMMA uprising destabilizes the film and leads to dewetting. Details of the dynamic dewetting process, i.e., the growth of fractal-like holes have been described elsewhere.[36] The fractal morphology is due to the anisotropy of the polymer mobility induced by the residual toluene solvent.[36] While in the case of lower swelling degree, the solvents disturb the film less and thus no dewetting occurred. The lateral nanostructure detected on the hills and valleys indicates that the hills and valleys did not result from lamellae being aligned parallel to the plane of the film. Local thickness adjusts to local minima of the free energy of the system which are related to energetically preferred microdomain structures in the film.[5,8]

Now, let us turn to the different nanostructures in the

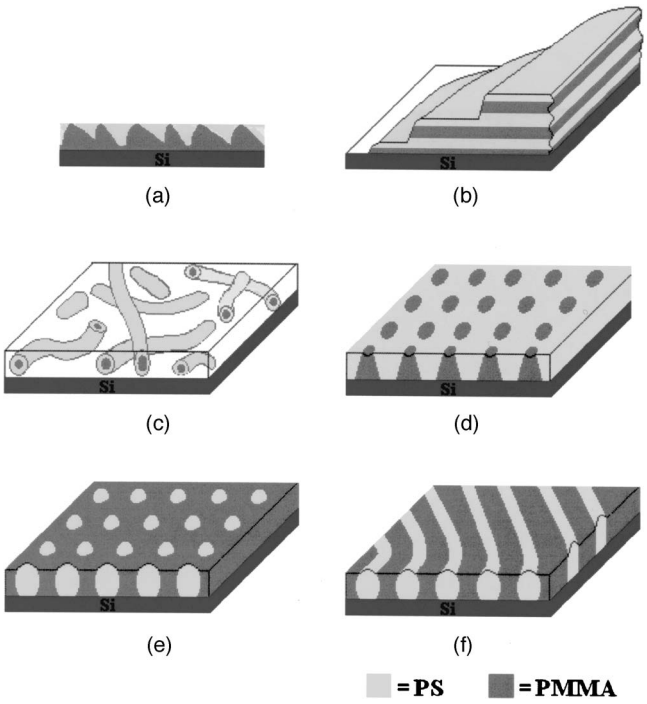

FIG. 5. Schematic representation of the microstructure of the as-cast film and subsequently annealed by different solvent vapors. (a) As-cast film, which shows PS dominates the free surface. (b) Upon exposure the film to THF, lamellae orient parallel to the interface. (c) When exposed to CS_2 selective for PS, PS forms a shield around the PMMA aggregates, resulting in the micellar structure. (d) When exposed to acetone selective for PMMA, in the case of higher swelling degree, PMMA blocks migrate upward and perforate the PS-rich layer, resulting in PMMA cylinders in PS matrix. (e) When exposed to acetone in the case of lower swelling degree, the aggregation of PS blocks to avoid contact with acetone overwhelms the PMMA upward attracted by acetone. As a result, PS blocks aggregate to form a spherical core surrounded by PMMA layer. (f) With further acetone annealing, the spherical PS domains merge with each other and form striped domains.

films with different swelling degrees. We have mentioned that when the as-cast PS-*b*-PMMA film was exposed to the acetone vapor, both PS and PMMA are swollen and can reconstruct themselves.[21] The PMMA blocks tend to perforate the PS-rich layer in response to the acetone attraction while the PS blocks tend to form aggregates with neighboring PS blocks to avoid contact with solvent. The thin film morphology formed is determined to a large extent by the competition between the PS and PMMA blocks which move faster, influenced by the swelling degree of the polymer films. In the case of higher swelling degree, the driving force that attracts PMMA upward is stronger. Therefore, the PMMA blocks perforate the PS-rich layer directly and migrate to the surface, resulting in hexagonal array of depressions [Fig. 5(d)]. Whereas in the case of lower swelling degree, the attraction of PMMA by acetone vapor is relatively weaker and therefore the aggregation of PS blocks dominates. The PS blocks aggregate to form a spherical core to avoid contact with acetone. The PMMA blocks form a layer around the PS core, resulting in an array of spheres [Fig. 5(e)]. With further acetone annealing, the spherical PS domains merge with each other and form striped domains [Fig. 5(f)].

V. CONCLUSIONS

The thin film structures of symmetric PS-*b*-PMMA diblock copolymer after annealing in neutral and different block-selective solvents are investigated. The nature of the solvent used for annealing is shown to have a significant influence on the structure formation. Upon neutral THF vapor annealing, PS and PMMA are equally swollen and terraces form exhibiting lamella oriented parallel to the surfaces. Upon PS-selective CS_2 vapor annealing, the PMMA blocks form aggregates while the PS blocks form a shield around the PMMA aggregates to avoid the PMMA-solvent unfavorable contact. Since the upper boundary condition still favors the PS, the PS will continue to dominate the upper surface. The solvent disturbs the film less and thus the film remains macroscopically flat. When using PMMA-selective acetone vapor annealing, the strong tendency of acetone molecules to attract the PMMA uprising destabilizes the film and leads to dewetting. In a nanometer scale, the PMMA blocks perforate the upper PS-rich layer and migrate to the surface in response to the acetone attraction, resulting in hexagonal array of depressions.

It is interesting to find that when decreasing the swelling degree of the film in the case of acetone vapor annealing, hills and valleys are observed in contrast to the dewetted morphology in the case of higher swelling degree. It is because in this case, the attraction of PMMA by acetone vapor is relatively weaker. The solvent disturbs the film less and thus no dewetting occurs. Hills and valleys form to adjust to the local minima of the free systematic energy. The PS blocks aggregate to form cores with PMMA blocks around, resulting in an array of spherical micelles. We note that, at present, the parameters characterizing the swelling degree of the film are only poorly controlled. Further work will have to concentrate on the proper experimental setups to systematically research the effects of temperature, vapor pressure, swelling degree of the film, etc., on the swelling process.

ACKNOWLEDGMENTS

This work is subsidized by the National Natural Science Foundation of China (20334010, 20474065, and 50573077). The authors are also grateful to Dr. Rüdiger Berger for his helpful discussion.

[1] F. S. Bates and G. H. Fredrickson, Annu. Rev. Phys. Chem. **41**, 525 (1990).
[2] M. J. Fasolka and A. M. Mayes, Annu. Rev. Mater. Res. **31**, 323 (2001).
[3] I. W. Hamley, *The Physics of Block Copolymers* (Oxford University Press, Oxford, 1998).
[4] L. Leibler, Macromolecules **13**, 1602 (1980).
[5] G. Coulon, V. R. Deline, P. F. Green, and T. P. Russell, Macromolecules **22**, 2581 (1989).
[6] K. Fukunaga, H. Elbs, R. Magerle, and G. Krausch, Macromolecules **33**, 947 (2000).
[7] K. Fukunaga, T. Hashimoto, H. Elbs, and G. Krausch, Macromolecules **35**, 4406 (2002).
[8] S. Ludwigs, K. Schmidt, C. M. Stafford, E. J. Amis, M. J. Fasolka, A. Karim, R. Magerle, and G. Krausch, Macromolecules **38**, 1850 (2005).
[9] S. H. Kim, M. J. Misner, T. Xu, M. Kimura, and T. P. Russell, Adv. Mater. (Weinheim, Ger.) **16**, 226 (2004).
[10] G. Kim and M. Libera, Macromolecules **31**, 2569 (1998).
[11] G. Kim and M. Libera, Macromolecules **31**, 2670 (1998).
[12] S. Niu and R. F. Saraf, Macromolecules **36**, 2428 (2003).

[13] P. Alexandridis and R. J. Spontak, Curr. Opin. Colloid Interface Sci. **4**, 130 (1999).
[14] B.-H. Sohn, S.-I. Yoo, B.-W. Seo, S.-H. Yun, and S.-M. Park, J. Am. Chem. Soc. **123**, 12734 (2001).
[15] Q. Zhang, O. K. C. Tsui, B. Du, F. Zhang, T. Tang, and T. He, Macromolecules **33**, 9561 (2000).
[16] H. Huang, F. Zhang, Z. Hu, B. Du, T. He, F. K. Lee, Y. Wang, and O. K. C. Tsui, Macromolecules **36**, 4084 (2003).
[17] Y. Chen, H. Huang, Z. Hu, and T. He, Langmuir **20**, 3805 (2004).
[18] J. Peng, Y. Xuan, H. F. Wang, Y. M. Yang, B. Y. Li, and Y. C. Han, J. Chem. Phys. **120**, 11163 (2004).
[19] Y. Xuan, J. Peng, L. Chi, H. F. Wang, B. Y. Li, and Y. C. Han, Macromolecules **37**, 7301 (2004).
[20] J. Peng, X. Gao, Y. Wei, H. F. Wang, B. Y. Li, and Y. C. Han, J. Chem. Phys. **122**, 114706 (2005).
[21] J. Peng, Y. Wei, H. F. Wang, B. Y. Li, and Y. C. Han, Macromol. Rapid Commun. **26**, 738 (2005).
[22] T. P. Lodge, K. J. Hanley, B. Pudil, and V. Alahapperuma, Macromolecules **36**, 816 (2003).
[23] K. J. Hanley, T. P. Lodge, and C.-I. Huang, Macromolecules **33**, 5918 (2000).
[24] C.-I. Huang, B. R. Chapman, T. P. Lodge, and N. P. Balsara, Macromolecules **31**, 9384 (1998).
[25] J. S. Pedersen, I. W. Hamley, C. Y. Ryu, and T. P. Lodge, Macromolecules **33**, 542 (2000).
[26] A. Choucair, C. Lavigueur, and A. Eisenberg, Langmuir **20**, 3894 (2004).
[27] Y. Yu and A. Eisenberg, J. Am. Chem. Soc. **119**, 8383 (1997).
[28] We estimated the repeat spacing of PS-*b*-PMMA lamellae in the kinetically trapped state from thin film morphology with perpendicular nanodomain orientation after annealing the film at $CHCl_3$ vapor for 100 h instead of the bulk equilibrium spacing in the thermodynamic equilibrium state using small-angle x-ray scattering (SAXS) due to experimental convenience.
[29] S. H. Anastasiadis, T. P. Russell, S. K. Satija, and C. F. Majkrzak, J. Chem. Phys. **92**, 5677 (1990).
[30] Ph. Leclère, G. Moineau, M. Minet, Ph. Dubois, R. Jérôme, J. L. Brédas, and R. Lazzaroni, Langmuir **15**, 3915 (1999).
[31] S. N. Magonov, V. Elings, and M. H. Whangbo, Surf. Sci. Lett. **375**, L385 (1997).
[32] J. P. Cleveland, B. Anczykowski, A. E. Schmidt, and V. B. Elings, Appl. Phys. Lett. **72**, 2613 (1998).
[33] *Polymer Handbook*, 4th ed., edited by J. Brandrup, E. H. Immergut, E. A. Grulke, A. Abe, and D. R. Bloch (Wiley, New York, 1999).
[34] A. Böker, A. H. E. Müller, and G. Krausch, Macromolecules **34**, 7477 (2001).
[35] S. H. Anastasiadis, T. P. Russell, S. K. Satija, and C. F. Majkrzak, Phys. Rev. Lett. **62**, 1852 (1989).
[36] J. Peng, Y. Xuan, H. F. Wang, B. Y. Li, and Y. C. Han, Polymer **46**, 5767 (2005).
[37] D. H. Kim, Z. Lin, H.-C. Kim, U. Jeong, and T. P. Russell, Adv. Mater. (Weinheim, Ger.) **15**, 811 (2003).
[38] T. Xu, J. T. Goldbach, M. J. Misner *et al.*, Macromolecules **37**, 2972 (2004).
[39] P. F. Green, T. M. Christenson, T. P. Russell, and R. Jerome, J. Chem. Phys. **92**, 1478 (1990).